Journal of Achievements in Materials and Manufacturing Engineering
VOLUME 57
ISSUE 1
March
2013

Numerical and experiment study of residual stress and strain in multi-pass GMA welding

R.R. Chand [a], I.S. Kim [b,*], J.P. Lee [b], Y.S. Kim [b], D.G. Kim [c]
[a] Mechanical Engineering, The University of the South Pacific, Suva, Fiji
[b] Department of Mechanical Engineering, Mokpo National University, 61, Dorim-ri, Chungkye-myun, Muan-gun, Chonnam, 534-729, Republic of Korea
[c] Mokpo Campus of Korea Polytechnic, 1854-16, Yeongsan-ro, Cheonggye-myeon, Muan-gun, Chonnam, 534-703, Republic of Korea
* Corresponding e-mail address: ilsookim@mokpo.ac.kr

Received 22.01.2013; published in revised form 01.03.2013

Analysis and modelling

ABSTRACT

Purpose: Recently, manufacturing industries have been concentrated on selection an optimal of welding parameter and condition that reduces the risk of mechanical failures on weld structures should be required in manufactory industry. In robotic GMA (Gas Metal Arc) welding process, heat and mass inputs are coupled and transferred by the weld arc to the molten weld pool and by the molten metal that is being transferred to the weld pool. The amount and distribution of the input energy are basically controlled by the obvious and careful choices of welding process parameters in order to accomplish the optimal bead geometry and the desired mechanical properties of the quality weldment. The residual stress and welding deformation have the large impact on the failure of welded structures.
Design/methodology/approach: To achieve the required precision for welded structures, it is required to predict the welding distortions at the early stages. Therefore, this study represented 2D Finite Element Method (FEM) to predict residual stress and strain on thick SS400 steel metal plate.
Findings: The experiment for Gas Metal Arc (GMA) welding process is also performed with similar welding condition to validate the FE results. The simulated and experiment results provide good evidence that heat input is main dependent on the welding parameter and residual stress and distortions are mainly affected by amount on heat input during each weld-pass.
Practical implications: This present study on based on the numerical analysis using ansys software, for a thick multi-pass GMA welding. A birth and death technique is employed to control the each weld pass welding.
Originality/value: The developed 2D multi-pass model employs Goldak's heat distribution, to simulate welding on SS400 steel butt-weld joint with a thickness of 16mm. moreover the numerical results are validated with experiment results.
Keywords: Residual stress; Strain; Finite Element Method; Ansys software; Robotic GMA welding

Reference to this paper should be given in the following way:
R.R. Chand, I.S. Kim, J.P. Lee, Y.S. Kim, D.G. Kim, Numerical and experiment study of residual stress and strain in multi-pass GMA welding, Journal of Achievements in Materials and Manufacturing Engineering 57/1 (2013) 31-37.

1. Introduction

GMA Automated welding is currently one of the most popular welding methods, especially in a broad range of industrial environments such as in areas of renewable energy. In GMA welding, heat source is created by an arc and maintained between a consumable electrode wire and work-piece. The weld is formed by melting and solidification of the filler material and base material. Inert gas is allowed to flow during the welding process to shield the weld metals from the surrounding atmosphere [1-6].

The local, non-uniform heating and subsequent cooling during the multi-pass welding process causes complex thermal stress/strain field to develop that finally leads to residual stress, distortion. The mechanical characteristics such as residual stress, distortion are prime concern to the industries producing weld-integrated structures around the world due to its obvious potential to cause inaccuracy in final welded structures [1]. Residual stress, develop in and around the welding zone are detrimental to the integrity and the service behaviour of welded structures. During the welding process, the weld area is heated up sharply compare to the surrounding area and fused locally. The material expands as a result of being heated [2]. The heat expansion is restrained by the surrounding cooler area, which gives rise to thermal stresses. To predict the magnitude and trends of residual stress and deformation fields is a complex phenomenon due to the involvement of various factors including short term localized heating and rapid cooling and metallurgical transformations [3].

There has been lot of experiment and FE being conducted to fully understand the welding temperature distribution and residual stress and also to predict welding quality. the most widely used the Goldak's double ellipsoidal heat source model could overcome the previous models and can simply and accurately simulate thermal elastic and plastic analysis for different type of welding processes[10-11].

Heinze et. al. [1] used 2D and 3D Goldak's double ellipsoidal heat source model to numerically calculate temperature field. A six bead multi-pass gas metal arc weld of 20 mm thick structural steel S355J2+N was simulated. This study also consider temperature-dependent material properties, phase transformations, "thermal" tempering, transformation plasticity, volume change due to phase transformation, an elastic–plastic material model, and isotropic strain hardening. Gery et al. [4] investigated the effects of the heat source distribution, energy input and welding speed on temperature variations in butt joint welding MIG welding processes using FE transient heat transfer analysis based on a double ellipsoidal moving heat source model.

A C++ program was developed in order to define a moving distributed heat source into simulations by using FE software Strand7. 3D and 2D FE models of plate butt welding processes were developed to predict the transient temperature distribution and variation of the welded plates during welding process. Deng et al. [5] developed 3D FE model and 2D axisymmetric FE model to analyze the temperature fields and the residual stress distributions for SUS304 stainless steel pipe based on ABAQUS S/W. Firstly, a 3D model was developed to simulate the temperature fields and welding residual stresses with a double ellipsoidal heat source. Secondly, based on the characteristics of the temperature fields and the welding residual stress fields, a 2D axisymmetric model was also developed using a volumetric heat source with uniform density. The results of both 3D model and 2D model were in very good with the experimental measurements.

Qureshi et. al [6] conducted a parametric studies for the effects of a critical geometric parameter, that is, tack weld on the corresponding residual stress fields in circumferentially welded thin-walled cylinders. Tack welds offer a considerable resistance to the shrinkage and the orientation, and size of tacks can alter altogether the stress patterns within the weldments. The results showed, that identical axial residual stress fields are observed on cylinders outer and inner surfaces for all the tack weld orientations under study with some exceptions on tack welds and weld start/stop locations. Liu. et. al [7] investigated pass-by-pass finite element (FE) simulation of residual stresses in narrow gap multi-pass welding of pipes with a wall thickness of 70 mm and 73 weld passes and also validated the residual stress on the outer surface with the experimental one. The results show that the residual stresses on the outer and inner surfaces are tensile in the weld zone and its vicinity. The through-wall axial residual stresses at the weld center line and the HAZ line demonstrate a distribution of bending type. The through-wall hoop residual stress within the weld is mostly tensile. After the groove is filled to a certain height, the peak tensile stresses and the stress distribution patterns for both axial and hoop stresses remain almost unchanged. Nguyen et al. [13] derived the analytical solutions for the transient temperature field of the semi-infinite body with conduction only consideration subjected to 3D power density moving heat sources such as semi-ellipsoidal and double ellipsoidal heat sources. The solution has been obtained by integrating the instant point heat source throughout the volume of the heat source. It was shown the analytical solution obtained for double ellipsoidal heat source was a general one that can be reduced to ellipsoidal, semi spherical, 2D Gaussian-distributed heat source and the classical instant point heat source.

Long. et. al [14] investigated distortions and residual stresses induced in butt joint of thin plates using Metal Inert Gas welding. This study used a moving distributed heat source model based on Goldak's double-ellipsoid heat flux distribution is implemented in Finite Element (FE) simulation of the welding process. Thermo-elastic–plastic FE methods were also applied to modelling thermal and mechanical behaviour of the welded plate during the welding process. It predicts of temperature variations, fusion zone and heat affected zone as well as longitudinal and transverse shrinkage, angular distortion, and residual stress. It also showed that the welding speed and plate thickness are shown to have considerable effects on welding distortions and residual stresses. De et al. [15] reported on a 2D axisymmetric FE analysis of heat flow during laser spot welding. This analysis was based on conduction heat transfer alone, but using the 'double ellipsoidal' representation of the laser beam. The extent of the beam is equal in both the front and the rear sections along the longitudinal direction and it seems to be sufficient to estimate the transition to keyhole formation during laser spot welding. Malik et al. [16] presented a computational procedure and techniques for the prediction of temperature distributions and the subsequent residual stress fields during the course of GTA welding of thin-walled cylinders of low carbon steel with the use of double ellipsoidal heat source model. A sequentially coupled, full 3D FE modeling was developed, in which transient, non-linear thermal solution based on heat conduction, convective and radiative boundary conditions was

first to solve for obtaining the temperature profiles. The temperature profiles were then used as thermal loads to obtain residual stress field. The accuracy of the developed model was validated for transient temperature distributions and residual stress fields through data measurement from experiments.

Therefore, the FE based numerical simulations attained a considerable important for the prediction of adverse consequences of complex multi-pass welding. In this study, a two-dimensioned finite element model developed to predict the residual stress and deformation in multi-pass GMA welding process. The developed model employs Goldak's heat distribution, to simulate welding on SS400 steel butt-weld joint with a thickness of 16 mm. Furthermore, FE results are validated with multi-pass experiment with similar welding condition as FE analysis.

2. Development of welding simulation model

In The GMA welding process is a coupled thermo-mechanical phenomenon is employed to evaluate the residual stress and deformations. Thus this coupled welding phenomenon can be split into thermal analysis followed by structural analysis. The finite element proceduce is presented in flow chart as shown in Fig. 1.

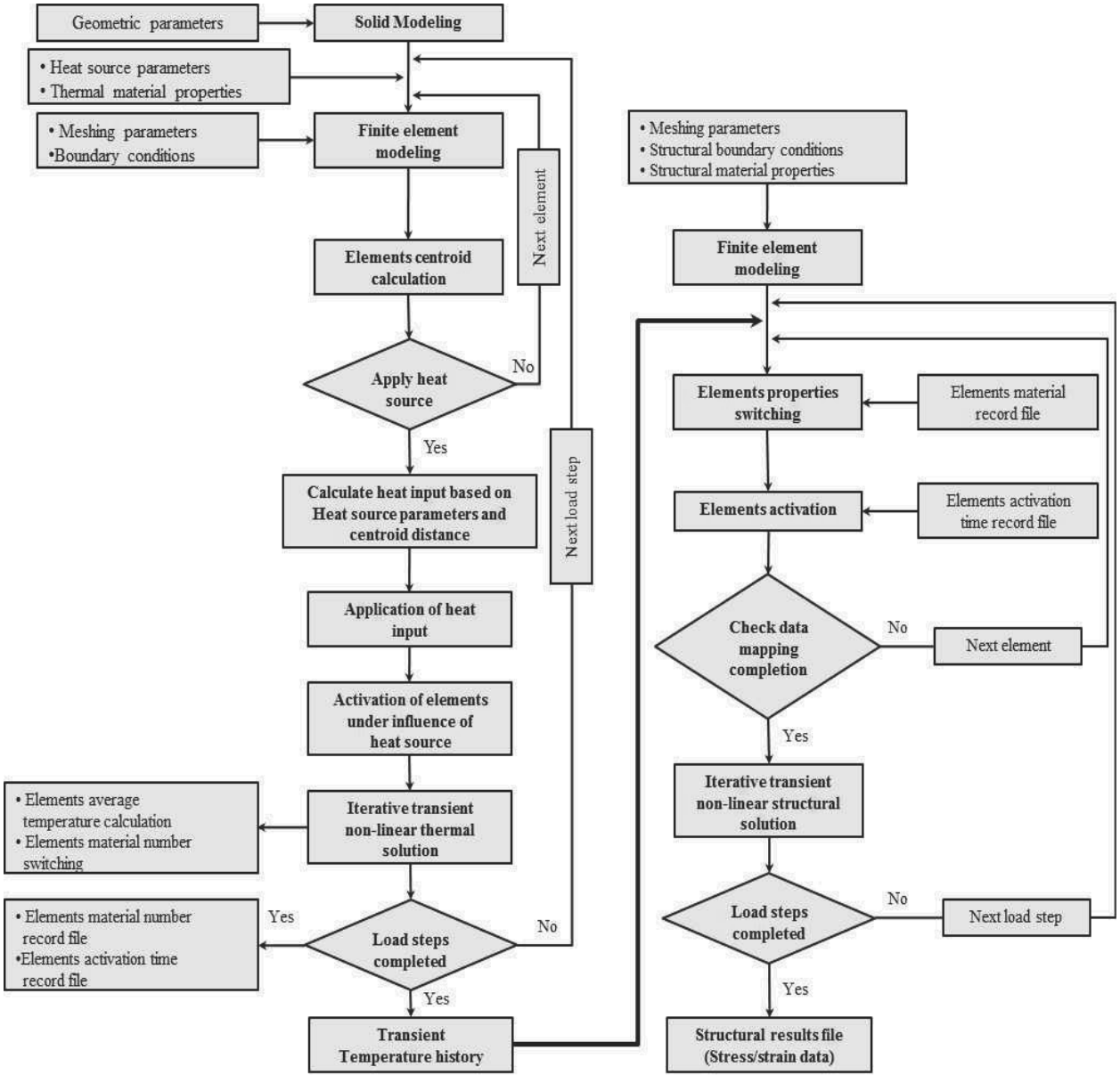

Fig. 1. Flow chart for FEM coupled thermo-mechanical phenomenon

2.1. Heat source model

The evolution thermal analysis is quite a complex phenomenon associated with GMA welding process. The weld pool shape can be largely influenced by the weld metal transfer mode and corresponding fluid flow dynamics [9]. In representation of GMA welding, the most widely acceptable double heat source model presented by Goldaks et al. [11] being used for the FE modeling as shown in Fig. 2.

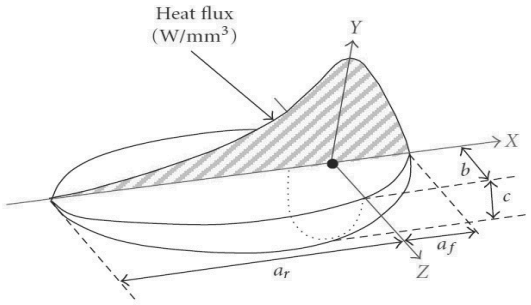

Fig. 2. Goldak's double ellipsoid heat source model [9]

The models give the Gaussian distribution for the butt and have excellent features of power and density distribution control in weld pool and HAZ. The Goldak's heat distributions are expressed by the following equations [10]:

$$q(x,y,z)=\frac{\sqrt[6]{3cQw}}{abc\pi\sqrt{\pi}}e^{-3x^2/a^2}e^{-3y^2/b^2}e^{-3z^2/c^2} \quad (1)$$

The parameter of moving heat source has been chosen to compute melted zone of thermal simulation and welding process parameter are listed in Table 1 and 2. In this simulation the each pass process parameter is different. The contribution of the transient temperature field is also temperature-dependent thermo-physical properties as shown in Fig. 3. Heat conduction problem has been solved using heat transfer analysis to obtain temperature histories. The combined heat transfer coefficient is expressed as follows;

$$h=24.1x10^4\varepsilon T^{1.61} \quad (2)$$

where ε is emissivity of the surface of the body, a value of 0.9 is assumed for this study [9].

Table 1.
Parameter of double ellipsoidal heat source

Weld pass	a(mm)	b(mm)	c_f(mm)	c_r(mm)	f_f	f_r
1	4.5	4.5	6	16	0.5454	1.4545
2	9	9	6	12.2	0.6593	1.3407
3	7	7	6	25	0.3870	1.6129
4	8.2	10	10.4	13.3	0.8776	1.1224
5	9.3	9.8	7.4	14.8	0.667	1.3333

Table 2.
Welding process parameters

Weld pass	Welding Voltage(V)	Arc Current (A)	Welding speed (mm/min)
1	23	200	11
2	26	280	
3	25	240	
4	25	260	
5	20	230	

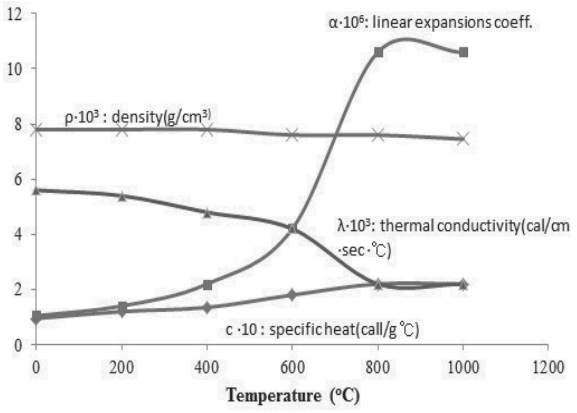

Fig. 3. Thermo-physical properties of SS400 steel as a function of temperature

The 2D thermal FE computational procedures has been developed to calculate the temperature histories for 5 bead multi-pass GMA welding process at different cooling time of SS400 steel. The dimension for five-pass finite element model is the 400mm in length and 16mm in thickness as shown in Fig. 4.

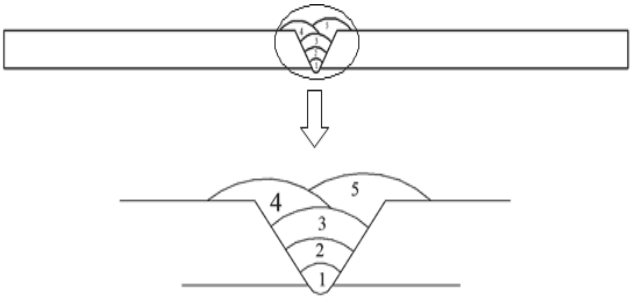

Fig. 4. Dimensional details and weld bead sequence for 5 pass butt weld

2.2. Structural Analysis

For mechanical analysis, the temperature history of each node from the preceding thermal analysis is input as the node load with temperature dependent mechanical properties shown in Fig. 5.

The von mises yield criteria is employed with σ1, σ2, and σ3 being the three principal stresses, coupled to a kinematic hardening rule,

$$\sigma_V = \sqrt{\frac{1}{2}[(\sigma_1 - \sigma_2)^2 + (\sigma_2 - \sigma_3)^2 + (\sigma_3 - \sigma_1)^2]} \quad (3)$$

The total strain can therefore be decomposed into three components as follows:

$$\varepsilon^{total} = \varepsilon^{e} + \varepsilon^{p} + \varepsilon^{th} \quad (4)$$

The component on the right-hand side of above equation corresponds to elastic, plastic and thermal strain, respectively.

The elastic strain is modeled using the isotropic Hooke's law with temperature-dependent Young's modulus and Poisson's ratio. For the plastic strain component, a plastic model is employed with the following features: the Von Mises yield surface and temperature-dependent mechanical properties.

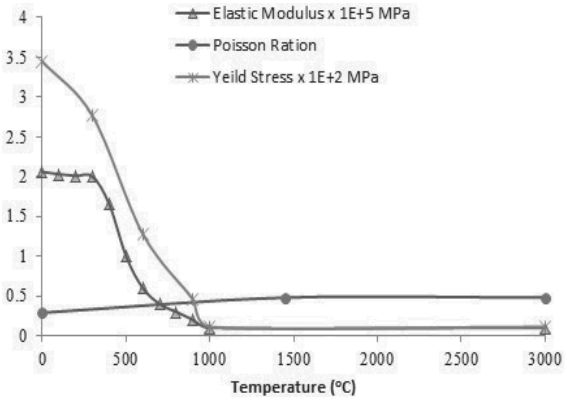

Fig. 5. Thermo-mechanical properties of SS400 steel as a function of temperature

3. Experimental procedure

To validate the FE model, a GMA welding experiment is conducted on 400×200×16 mm thick SS400 steel with similar geometry and welding process parameters from the FE model as shown in Fig. 6. Commercial high-tech, fully automatic GMA M500S welding equipment along with automated wire feeder and welding fixtures were used to reflect the desired structural boundary conditions. Five pass butt-weld geometry is used with single "V" groove having included angle of and 5mm root opening same as FE model as indicated in Fig. 2. The welding carriage is moved with a constant welding speed alone the rails.

A non-destructive, x-ray diffraction measurement methods is used to measure residual stress across the welded plate. It uses the interatomic spacing as the ultimate gage length, the X-ray technique is ideal for and applicable to all crystalline materials, especially for metals, but also for ceramics. In addition to the FE parameters, carbon dioxide was used as shielding gas with flow rate of 20 liter/min.

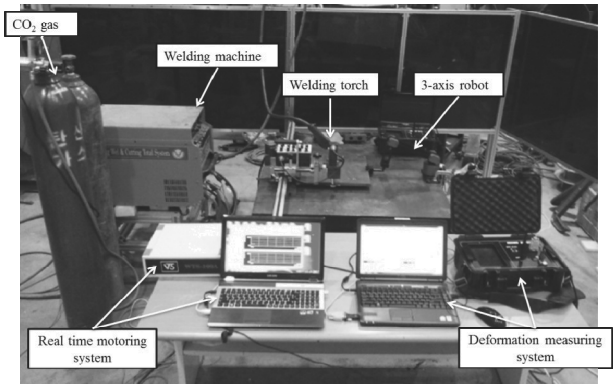

Fig. 6. Multi-pass GMA welding experiment setup

4. Results and discussion

The multi-pass weld is quite challenging due its differential heat input and cooling time, to maintain the temperature after each pass to be 100°C. Fig. 7 shows the FE simulated and experimental bead geometry, similar pattern of geometry is observed on experimental bead geometry compared to the FE analysis.

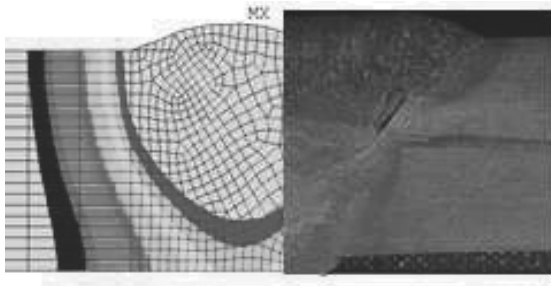

Fig. 7. Comparison of FE simulation and experimental bead geometry

Fig. 8 shows the FZ and HAZ temperature distribution from FEM analysis. After each weld pass the material is allowed to cool down to about 100°C, to maintain the temperature of base material same before proceeding another weld pass, therefore each weld pass has different time of cool. The peak temperatures at each pass are different due to difference in welding parameters.

Repeated heating and subsequent cooling has a large impact on the residual stress of the base material during multi-pass welding process. Tensile and compressive residual stress fields are observed near the weld region based on different temperature distribution on the plate. The different temperature gradient results at the top surface and bottom surface produce different tensile and compressive residual stress and varying the shrinkage patterns through the thickness of the butt welded plate. The transverse and longitudinal stress distribution along the width at the top surface of the plate is shown in Fig. 9(a,b). Fig. 9a compares the FM simulation and experimental transverse residual stress, a similar pattern and transverse residual stress and experimental measured residual but there is quite difference in

magnitude of the stress. From FE simulation results, it can be observed that around HAZ a tensile stress while at FZ and actual welding region is under compressive residual stress.

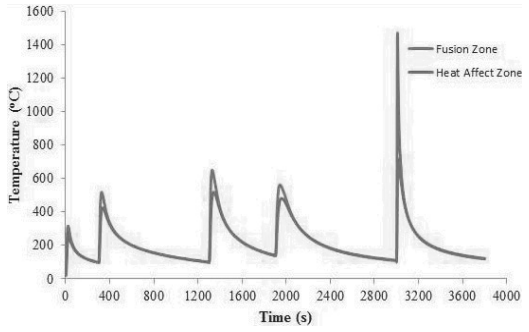

Fig. 8. FEM FZ and HAZ Temperature histories of each pass for multi-pass welding

a)

b)

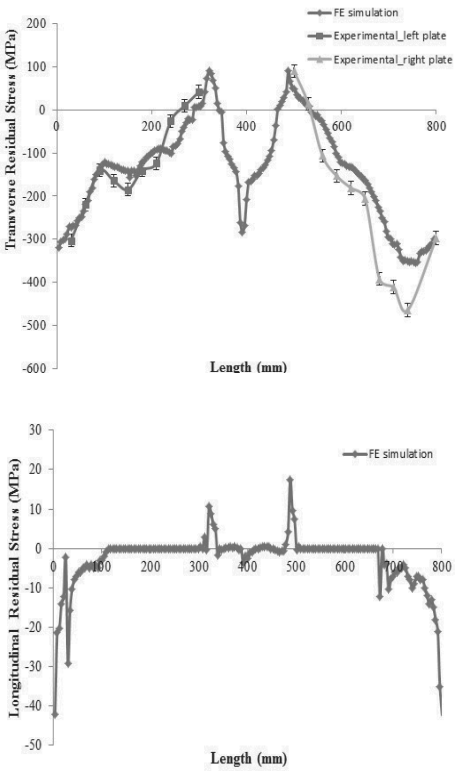

Fig. 9. Transverse and Longitudinal residual stress at the top surface of the weld plate, a) Transverse residual stress. b) Longitudinal residual stress

The edge of the plate and at welding region, a compressive longitudinal residual stress is observed whereas at the HAZ the tensile residual stress. In FZ the stress fluctuate from compressive to tensile stress on the left side of the plate. The residual stress magnitude and distribution at the bottom surface is different compared to top surface due to the groove joint and also weld pass 3, 4 and 5 has large impact on top surface. The transverse residual stress at HAZ is observed to compressive initially but as moved further toward welding region the stress becomes tensile. The large compressive stress is noted at the weld region and FZ as shown in Fig. 10(a). Fig. 10(b) shows longitudinal residual stress at the bottom surface to butt welded plate. At HAZ and FZ the compressive stress and tensile stress is observed.

Fig. 11(a) shows the transverse strain distribution on the plate. It can be observed that the transverse strain distribution at HAZ and FZ is mainly concentrated as tensile strain on the left side plate and at the welding region the strains fluctuate from tensile to compressive. Fig. 11(b) also shows that strain at right side plate are under compressive. The elastic strain at left and right side plate varies due to left side plate being restrained and due to difference in heat load which is applied to the four and five weld-pass. For longitudinal strain, it is observed that the top surface of the plate, have tensile strain at HAZ, whereas at FZ and in vicinity of welding region it has compressive strain.

a)

b)

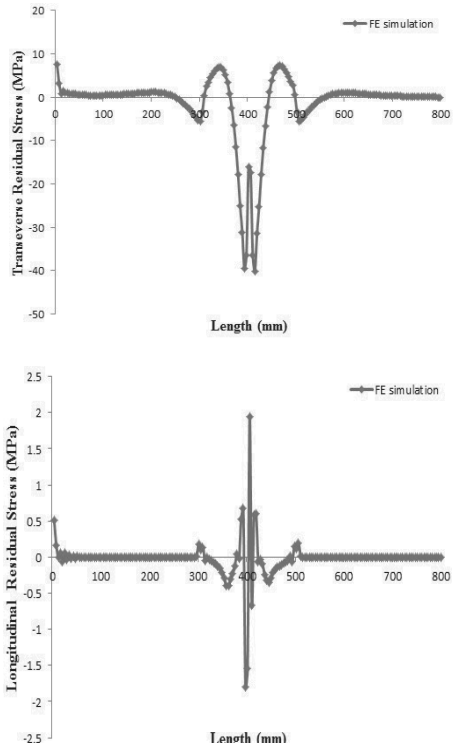

Fig. 10. Transverse and Longitudinal residual stress at the bottom surface of the weld plate, a) Transverse residual stress, b) Longitudinal residual stress

5. Conclusions

2D FE simulations of five pass GMA welding was performed on the 16mm thick SS400 material, to determine residual stress, strain and deflection on the plate. The FE simulation results are verified by experimental results with similar weld conditions and geometry. According to the numerical and experimental analysis results, the following conclusion can be drawn.

a)

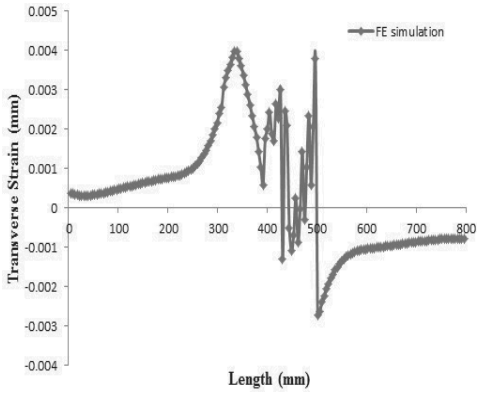

b)

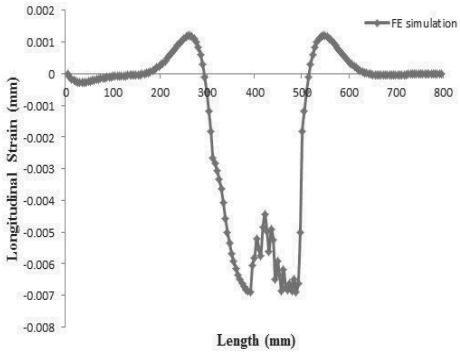

Fig. 11. Transverse and longitudinal strain distribution on the welded plate, a) Transverse stress, b) Longitudinal stress

1. Based on the simulation results, The heat input and peak temperatures of weld pool are depend on the welding process parameter, voltage and current and travelling speed of welding touch, whereas temperature distribution, residual stress and deformation are dependent thermal material properties, heat input, the cooling rate and restrains on the plate.
2. It is know that residual stress and strain distribution on top and bottom surface of the plate differs, due to heat distribution load applied to plate, the heat input and also the cooling time after each welding pass. The restraint of plate has also impact on residual stress and strain. The FEM results have much resemblance with the experimental residual stress pattern and magnitude.

Acknowledgements

This research was financially supported by the Ministry of Education, Science Technology (MEST) and National Research Foundation of Korea (NRF) through the Human Resource Training Project for Regional Innovation.

This work (Grants No. C0002256) was supported by Business for Cooperative R&D between Industry, Academy, and Research Institute funded Korea Small and Medium Business Administration in 2012.

References

[1] C. Heinze, C. Schwenk, M. Rethmeier, Numerical calculation of residual stress development of multi-pass gas metal arc welding under restraint conditions, Materials and Design Materials and Design 35 (2012) 201-209.
[2] D. Deng, FEM prediction of welding residual stress and distortion in carbon steel considering phase transformation effects, Materials and Design 30/2 (2009) 359-366.
[3] D. Deng, H. Murakawa, Prediction of welding distortion and residual stress in a thin plate butt-welded joint, Computational Materials Science 43 (2008) 353-365.
[4] D. Gery, H. Long, P. Maropoulos, Effects of welding speed, energy input and heat source distribution on temperature variations in butt joint welding, Journal of Materials Processing Technology 167 (2005) 393-401.
[5] D. Deng, W. Liang, H. Murakawa, Determination of welding deformation in fillet-welded joint by means of numerical simulation and comparison with experimental measurements, Journal of Materials Processing Technology 183/2-3 (2007) 219-225.
[6] E.M. Qureshi, A.M. Malik, N.U. Dar, Residual stress fields due to varying tack welds orientation in circumferentially welded thin-walled cylindersinternational, Journal of Advances in Mechanical Engineering (2009).
[7] C. Liu, J.X. Zhang, C.B. Xue, Numerical Investigation on residual stress distribution and evolutions during multi-pass narrow gap welding of thick-welled stainless steel pipes, Journal of Fusion Engineering and Design 86 (2011) 288-295.
[8] Sattari-Far, Y. Javadi, Influence of welding sequence on welding distortions in pipes, International Journal of Pressure Vessels and Piping 85/4 (2008) 265-274.
[9] J.A. Goldak, M. Akhlaghi, Computational welding Mechanics Springer, 2005.
[10] J. Goldak, M. Bibby, J. Moore, R. House, B. Patel, Computer modeling of heat flow in welds, Metallurgical Transactions B 17/3 (1986) 587-600.
[11] J. Goldak, A. Chakravarti, M. Bibby, A new finite element model for welding heat source, International Journal Metallurgical and Materials Transactions B 15/2 (1984) 299-305.
[12] P. Duranton, J. Devaux, V. Robin, P. Gilles, J.M. Bergheau, 3D modeling of multi-pass welding of a 316L stainless steel pipe, Journal Materials Processing Technology 153-154 (2004) 457-463.
[13] N.T. Nguyen, T.A. Ohta, K. Matsuoka, N. Suzuki, Y. Maeda, Analytical solutions for transient temperature of semi-infinite body subjected to 3-D moving heat sources, Welding Journal (1999) 265-274.
[14] H. Long, D. Gery, A. Carlier, P.S. Maropoulos, Prediction of welding distortion in butt joint of thin plates, Jounral of Material and Design 30 (2009) 4126-4135.
[15] De, S.K. Maiti, C.A. Walsh, H.K.D.H. Bhadeshia, Finite element simulation of laser spot welding, Science and Technology of Welding and Joining 8 (2003) 377-384.
[16] A.M. Malik, E.M. Qureshi, N.U. Dar, I. Khan, Analysis of circumferentially arc welded thin-walled cylinders to investigate the residual stress fields, Thin-Walled Structures, 46/12 (2008) 1391-1401.
[17] Z.B. Dong, Y.H. Wei, Three dimensional modeling weld solidification cracks in multi-pass welding, Theoretical and Applied Fracture Mechanics 46/2 (2006) 156-165.
[18] D. Deng, H. Murakawa, W. Liang, Numerical simulation of welding distortion in large structures, Computer Methods in Applied Mechanics and Engineering 196 (2007) 4613-4627.